

# Integrity of Composite Aircraft Fuselage Materials under Crash Fire Conditions.

G. LA DELFA, J. W. LUINGE\*, A. G. GIBSON

*NewRail Centre for Railway Research, Stephenson Building  
University of Newcastle upon Tyne, NE1 7RU, UK*

*\*EADS Innovation Works. TCC1/ Department IW-CT, 81663, Munich, Germany.*

## ABSTRACT

This paper summarizes a series of small-scale tests carried out to evaluate and model the post-crash fire integrity of composite aircraft fuselage structures.

The US Federal Aviation Administration regulations for the penetration of an external fuel fire into an aircraft cabin after crash require a burn-through period of 4 minutes (FAA § 25.856 Appendix F, Part VII). Different candidate structures for the next generation of composite aircraft fuselage, provided by Airbus, were investigated, including CFRP monolithic laminate and a folded-core CFRP sandwich. Those materials were subjected to constant heat flux from a propane gas burner, while being held under compressive load in a small, specially designed compression test rig with anti-buckling guides. The propane burner was calibrated to produce a constant heat flux up to 182 kW/m<sup>2</sup>. The sample time-to-failure was measured, along with the temperatures at various points through the thickness.

Modelling the thermal and structural behaviour under load required the use of a modified version of the Henderson Equation, which describes heat transfer through composites under ablative fire conditions. This has been incorporated into the Com-Fire software model. Kinetic parameters for the resin decomposition reaction were determined from thermo-gravimetric data and other thermal parameters, conductivity and diffusivity were measured experimentally. The paper will compare the behaviour of single and double-skinned structures and will examine measured and modelled behaviour.

## 1. INTRODUCTION

This paper describes small-scale tests and a model to evaluate the integrity of composite aircraft materials exposed to fire conditions [1]. In the past decade there has been rapid development of polymer composite materials in aircraft due to the strength, stiffness and lightweight advantages. This trend is expected to continue in the future as these materials are replacing aluminium and other aerospace alloys in the primary structure and control surface [2]. One question that needs to be asked, however, is whether the growing use of polymer composite materials has increased the fire hazard due to the flammable nature of the organic matrix. Hence a serious situation known as “Post crash fire condition” has to be considered since this has important consequence during many accidents. As shown in Table I the Civil Aviation Authority (CAA) reported that “Collision with terrain/water/obstacle” was a consequence in 47% of accidents, whilst “Controlled flight into terrain (CFIT)” was a consequence in 35% of accidents. “Post crash fire” involves 22% of the total accidents [3].

Table I. Consequences of fatal civil aircraft accidents:

	Fatal accidents	
1) Collision with terrain / water / obstacle	289	(46.5%)
2) Controlled flight into terrain (CFIT)	219	(35.3%)
3) Loss of control in flight	178	(28.7%)
4) Post crash fire	134	(21.6%)
5) Overrun	55	(8.9%)
6) Undershoot	53	(8.5%)
7) Ground collision with object / obstacle	39	(6.3%)
8) Forced landing - land or water	30	(4.8%)
9) Structural failure	27	(4.3%)
10) Fire/smoke during operation	24	(3.9%)

*Note: The consequences are not mutually exclusive as each accident generally involved more than one consequence.*

Two important factors are considered in this paper: burn-through resistance and structural integrity. The fuselage burn-through refers to the penetration of an external post-crash fuel fire into an aircraft cabin. In survivable aircraft accidents the time to burn-through is critical because of the hazard associated with burning cabin materials which have been ignited by external fuel fire. This may incapacitate passengers due to smoke inhalation and lack of oxygen before they are able to escape from the aeroplane. The goals set by the Federal Aviation Administrative (FAA) state that during passenger evacuation the flame penetration should not reach the cabin interior 4-5 minutes after a crash. Also, the fuselage structure should have a low heat release rate and sufficient structural integrity. The fire response requirements by the FAA are that the maximum heat release rate during a five minute test will not exceed  $65 \text{ kW/m}^2$  and the total heat released during the first 2 minutes will not exceed  $65 \text{ kW min/m}^2$  [4].

## 2. MATERIALS AND EXPERIMENTAL

### 2.1 Materials:

Two types of material construction were investigated. The first was a Carbon Fibre Reinforced Polymer CFRP not-isotropic monolithic laminate (Figure1). Two separate laminate thicknesses were considered (2.1 mm and 1.7 mm thickness). The second material construction considered a sandwich panel (Figure2). The skins of which were made from the same CFRP construction as described previously. The core which was adhesively bonded to the skins was made from “folded mechanical paper and phenolic resins”. The laminate skins have good mechanical characteristics compared with the weak core. In addition, the core gives good thermal insulation properties. The main drawbacks are susceptibility to buckling and lack of resistance to penetration of sharp objects.



Figure 1. CFRP carbon epoxy laminate

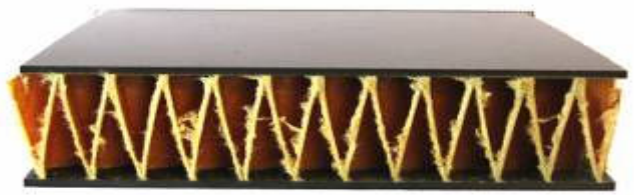


Figure 2. Folded core CFRP sandwich panel

### 2.2 Thermo-gravimetric Analysis (TGA)

The thermal model required certain kinetic parameters in order to calculate the rate of decomposition of the composite resin. Thermo-gravimetric analysis was used in this work to study the degradation kinetics of the epoxy matrix. The TGA was performed in a nitrogen atmosphere at three heating rates of  $5^\circ\text{C/min}$ ,  $10^\circ\text{C/min}$  and  $20^\circ\text{C/min}$ . The TGA measured the mass loss of the materials with increasing temperature, this could then be correlated to the amount of decomposition. After that the decomposition reaction rate constants A, E and n are determined. The procedure is explained in more detail in the next paragraph 4.1.

### 2.3 Fire under Compression Load Test

Compression performance of advanced composites is a limiting design parameter. While tensile performance of carbon fibres has continued to increase, the compression performance has remained relatively stagnant for a wide variety of fibre types and diameters. For this

reason the specimens were tested in compression. Fire testing under load were carried out on small scale samples. A propane burner was used to produce a constant heat flux of  $75\text{kW/m}^2$  and also  $182\text{ kW/m}^2$  to the front face. As well as measuring the time to failure, the temperatures at different points through the thickness also was recorded. These results were used to validate the CFRP laminate compressive strength model predictions [7-10]. Figure 3 shows the test method. Anti-buckling guides were set up to avoid the column failure mode. This type of system is comparable with the well-known Boeing compression test [11]. The lateral constraints raised the load required for buckling failure, this enabled specimens of reasonable size to be placed under significant compressive stress during the fire tests. The material outside the heated region and the back surface were not insulated with a thermal blanket to simulate a real circumstance.

Two important parameters were needed in order to maintain a constant heat flux: the distance from the burner to the sample and the pressure of gas to the burner was held constant.

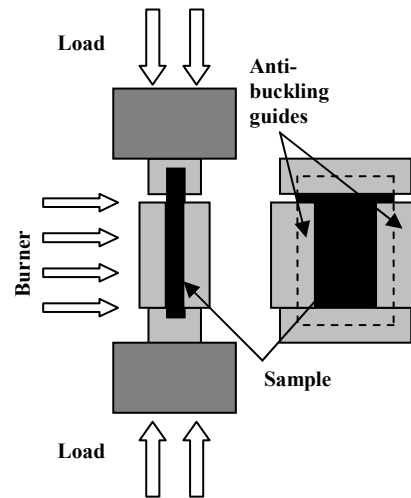


Figure 3. Propane Burner Test

#### 2.4 Thermal Diffusivity measurements

The thermal model required calculation of some thermal parameters to give accurate prediction of the fire response of the polymer composite. In particular, the thermal conductivity of the materials was calculated with the following relation:

$$k = \rho C_p \alpha \quad (1)$$

where  $\rho$  is density,  $c_p$  is specific heat and  $\alpha$  is thermal diffusivity.

The density was taken to be  $1310\text{ kg/m}^3$  and the specific heat as  $1278\text{ J/kg}^\circ\text{K}$ . Laplace's equation can be used to form a model for unsteady state heat flow:

$$\frac{dT}{dt} = \alpha \cdot \frac{d^2T}{dx^2} \quad (2)$$

The model considered the temperature of the centre of a slab at the point the sample was removed from the oven,  $T_0$ , and also while the sample cooled to a lower temperature  $T_1$ . Equation (2) can be expanded to describe the behaviour of the heat flow as follows:

$$\frac{T - T_0}{T_1 - T_0} = 1 - \frac{4}{\pi} \exp\left(\frac{-\pi^2 F_0}{4}\right) \quad (3)$$

$$F_0 = \frac{\alpha \cdot t}{b^2} \quad (4)$$

$F_0$  is Fourier number,  $t$  is the time in (sec) and  $b$  is the thickness of the specimen (mm). The cooling was measured experimentally, submerging the sample in water and recording the variation of temperature from 50°C to 15°C. Once the experimental cooling curve was obtained, this was then super imposed over the curve obtained from the model. The value of  $\alpha$  thermal diffusivity was then manually altered in order to best fit the actual results. Finally the thermal conductivity was calculated using equation (1).

### 3. RESULTS AND DISCUSSION:

#### 3.1 Fire Test under Compressive Load

Fire tests under compressive load have been carried out on the CFRP NI (not isotropic) laminate specimens and on the folded-core sandwich with different skin thicknesses. The specimens were subjected to a constant compressive load with one side exposed to fire using a propane burner. The loads were applied to the specimens using a 295kN hydraulic machine. The specimens, in the vertical position, were exposed to a calibrated high heat flux of 182 kW/m<sup>2</sup>. The distance of the propane torch to the surface of the panel was 35 cm.

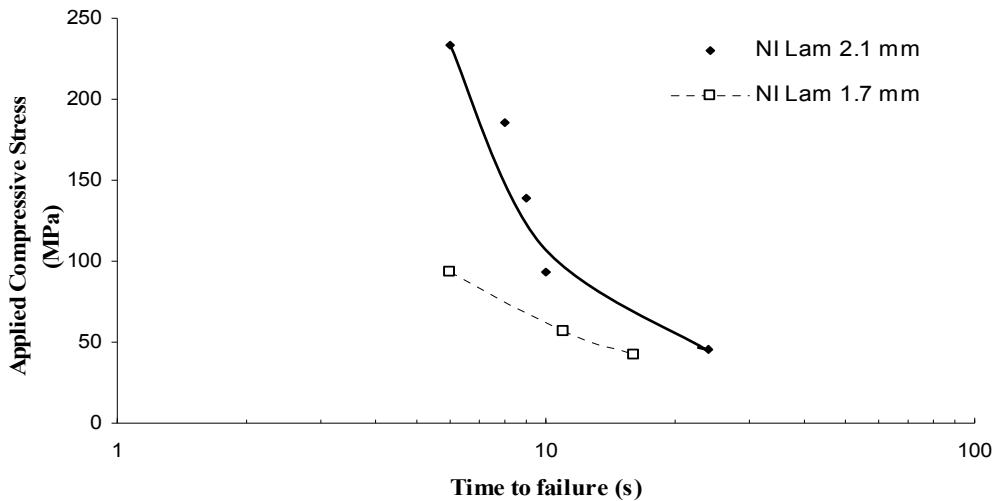


Figure 4. Failure times for CFRP carbon epoxy laminates at different thickness exposed to an heat flux of 182 kW/m<sup>2</sup>.

The time to failure was recorded. This was defined as the time needed for the exposed face to fail. In preliminary experiments CFRP NI laminates have been studied. The results of this study indicate that the failure time for the laminates are very short. Figure 4 shows that this ranged from 8 to 15 secs. It is apparent from the graph below that the time to failure increased with the laminate thickness. These results are consistent with those of other studies [12]. The most likely form of failure found seems to be delamination between the plies nearest the hot surface.

The burn-through resistance was considered on the basic that no flame should penetrate on the back face before 4-5 minutes. Laminates reasonably withstand high temperatures; however, the burn-through resistance gives better performance with sandwich panels. Therefore more consideration will be given to the burn through thickness resistance of the sandwich panel.

The constant compressive stress was applied on both skins until failure of the samples occurred. Different failure modes arose depending on the size of the applied compressive stress. When the stress was high the time to failure was short as shown in Figure 5.

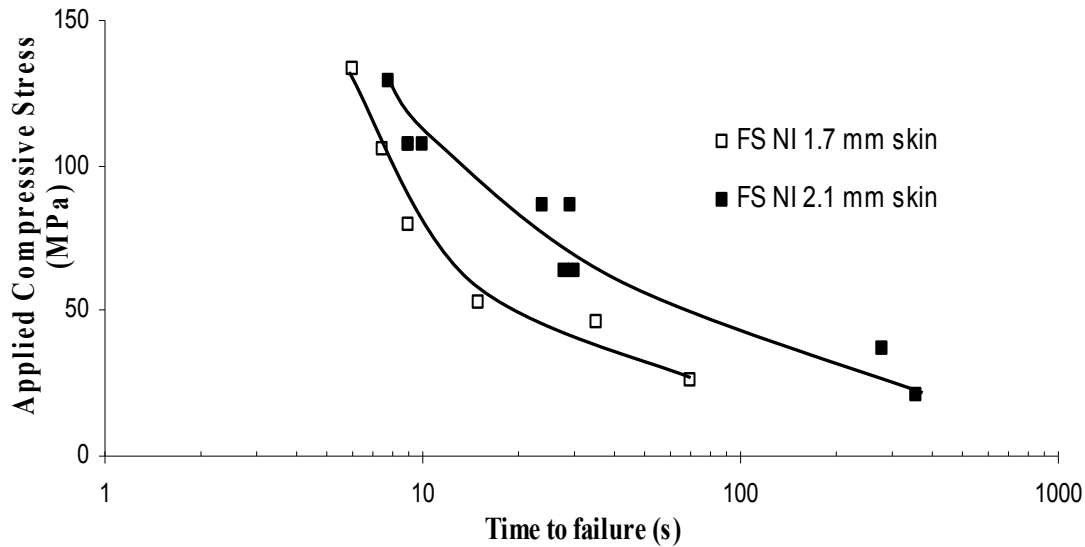


Figure 5. Failure times for sandwich composite with CFRP carbon epoxy skins at different thickness exposed to a heat flux of  $182 \text{ kW/m}^2$ . The compressive load was applied in both skins.

Mainly the failure mode involved collapse of the front skins with little delaminations and kinking of the ply [13-14]. This can be observed in Figure 6 below. The fibres were broken at each kink band boundary. Failures predominantly occurred in the centre of the specimens. At the boundary the main failure mode was local buckling.

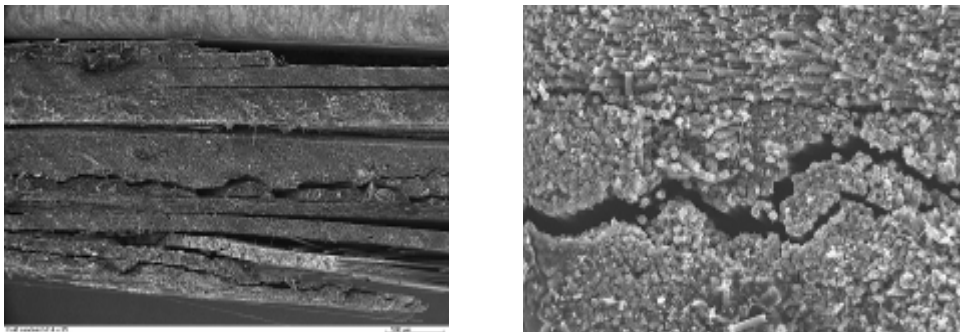


Figure 6. Scanning Electron Microscopy of CFRP carbon epoxy skins exposed to an heat flux of  $182 \text{ kW/m}^2$  and compressive load. Formation of delaminations due to the accumulation of volatile gas. Enlarged view of the carbon epoxy delaminations on the right side picture.

A different mode of failure was observed when the stress was very low. Failure occurred over a longer period of time. The main failure mode noted was debonding of the front skins from the core materials for both thickness of the FS NI sandwich panel. A possible explanation for this might be that since the load was very low, the skins were unaffected and the thin adhesive subjected at high temperature and load failed. The time to failure of the sandwich panels with thicker skins response was 3 time more than the thinner ones at medium-low load. The burn-through resistance was successful as the sandwich was able to withstand the flame for 4-5 minutes as FAA regulations required.

The experiment for the sandwich panels was repeated under different conditions in which the specimens were reduced in length by 2 mm per sides. The purpose of this modification was that the skin unexposed to fire should carry out all the stress. This implies that the front skin was subjected only to fire. The time to failure was recorded when the back skins failed. The results of this part of analysis led to the conclusion that the panels lasted longer time than the

previous method as shown in Figure 7. The mode of failure recognized a kink band broadening without fibre fracture on the internal skins with debonding of the core from the exposed skins. This was accompanied with evidence of structural buckling and delaminations. Further research should be done to investigate the failure of the unexposed skin.

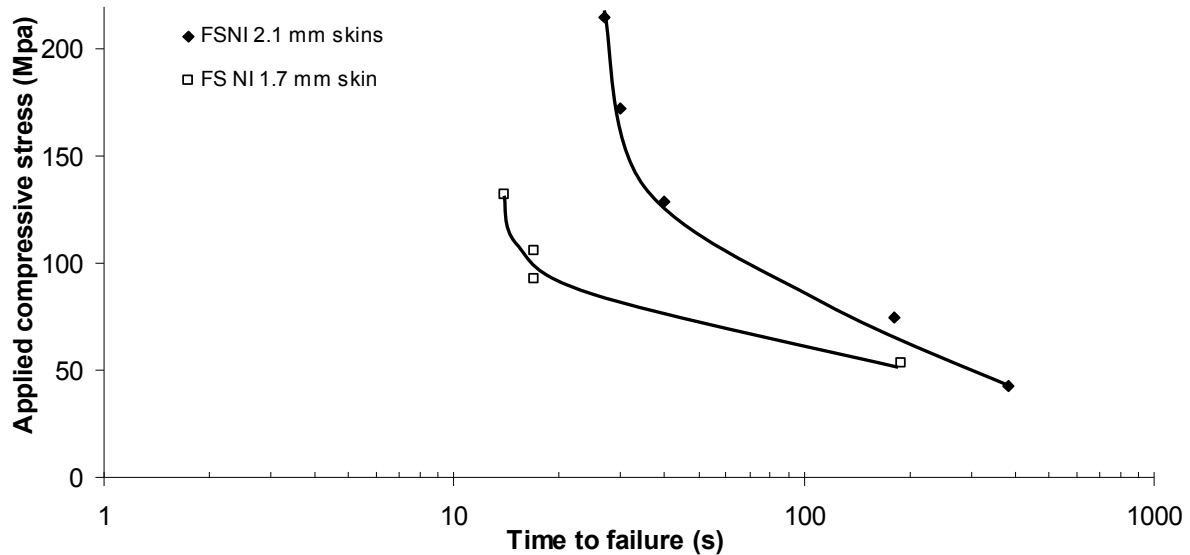


Figure 7. Failure times for sandwich composite with CFRP carbon epoxy skins at different thickness exposed to a heat flux of  $182 \text{ kW/m}^2$ . The compressive load was applied only on the skin not exposed to fire.

### 3.2 Thermal Diffusivity measurement

The thermal diffusivity was calculated recording the variation of temperature from  $50$  to  $15$   $^{\circ}\text{C}$  which was the water temperature. A thermocouple was embedded in the middle between two faces of the specimens. The setup procedure was the same for a Macor glass ceramic, CFRP NI laminate and sandwich panels. For the latter, two thermocouples were used.

The materials were surrounded with adhesive tape to prevent water intrusion. To achieve the required temperature, testing was performed using an oven. After thermal equilibrium was achieved, the specimens were dipped in water and cooling rate was recorded.

Validation of the test method was carried out using Macor glass ceramic. The thermal conductivity of which was given as  $1.46 \text{ W/m}^{\circ}\text{K}$ . The dimensions of the specimens were: length  $50 \text{ mm}$ , width  $50 \text{ mm}$  and  $20 \text{ mm}$  thickness. The results obtained from the analysis for Macor glass ceramic shown a significant positive correlation between the predictive and experimental curves. The response showed that the thermal conductivity  $K$ , was  $1.43 \text{ W/m}^{\circ}\text{K}$  at  $50$   $^{\circ}\text{C}$ . This was less than  $3\%$  lower than the one given from the supplier.

Tests were conducted on the laminate and on the sandwich panels with  $2.1 \text{ mm}$  skins thickness. The dimensions of the specimens were standard as previous described. The laminate thickness was  $2.1 \text{ mm}$ , and  $34 \text{ mm}$  for the sandwich panels. Good agreement exists between the experimental and the calculated temperatures variation for the CFRP single skin laminate and the sandwich panels as shown in Figure 8. The response was that the thermal conductivities  $K$  obtained was  $0.21 \text{ W/m}^{\circ}\text{K}$  at  $50$   $^{\circ}\text{C}$  for the 977 laminate and  $0.05 \text{ W/m}^{\circ}\text{K}$  for the sandwich panels. The most important limitation lies in the fact that this method cannot be used at higher temperature higher than  $50^{\circ}\text{C}$  because comparison between experimental and prediction was not well correlated.

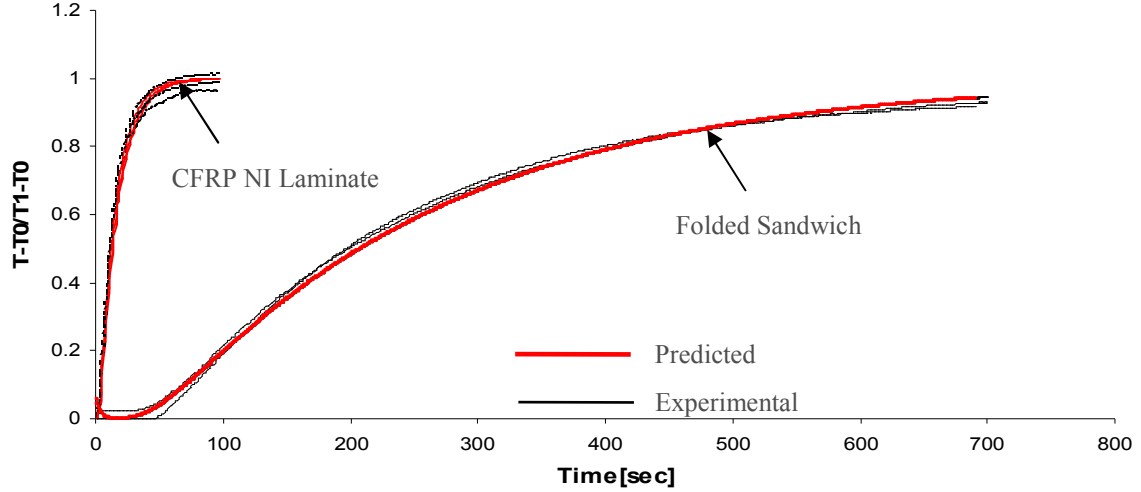


Figure 8. Variations of temperature with time for the CFRP NI epoxy laminate and the sandwich panel.

## 4. MODELLING AND RESULTS:

### 4.1 Analysis TGA

The degradation of linear polymers is a complex phenomenon and although many authors have studied it, many aspects are still unclear [15-17]. Analysis and comparison of the TGA curves allowed the calculation of the reaction rate factor (A) and activation energy (E) for each material. The general form of the kinetic expression to analyse the dynamic TG data was based on the  $n^{\text{th}}$  order of the reaction mechanism and the temperature dependence could be sufficiently described by the Arrhenius equation which is written in the following form:

$$\frac{d\alpha}{dt} = -A \cdot e^{-\frac{B}{T}} \left( \frac{m - m_f}{m_o - m_f} \right)^n \quad (5)$$

where:  $d\alpha/dt$  is the rate of change of mass (kg/s), A is the rate constant (1/s),  $m_o$ , m and  $m_f$  are the original, instantaneous and final mass of the polymer during the decomposition process (kg),  $B=E/R$  where E is the activation energy (J/mol), R is the universal gas constant (8.314 J/mol K), T is the temperature (K), n is the order of the reaction.

From the results two stages of reaction are evident. The first was a volatile process occurred over the temperature interval of 350 to 450 °C. The second was a decomposition of the non-volatile residues formed in the first stage occurred from 450 to 520 °C. The maximum rates of weight loss were 0.08, 0.15 and 0.29 per minute respectively for 5, 10 and 20 °C /min heating rates. Both mass loss curves had the same shape, however the different heating rates produced an effective shift in the temperature around which most of the decomposition occurred.

A linear first order decomposition reaction type was observed, which accounted for the major degree of decomposition region between 0.26 to 0.85. From a preliminary analysis a value of B was found from the slope of  $\ln \dot{\alpha}$  versus  $1/T$  (°K) (Fig.9). A dozen values of  $\alpha$  were selected ranging from 0.4 to 0.8. Values of  $\dot{\alpha}$  (rate of reaction) and T were determined from each heating rates. As shown in Table II, the correlation coefficient is always greater than 0.997 when  $0.4 < \alpha < 0.8$ . The evolution of the activation energy was noted by a lower value at the beginning of the degradation. Further analysis showed that an initial  $E_a$  value was about 93 kJ/mol. In addition to the resin degradation parameters, the heat of combustion and order of reaction, n, were required for each material. The heat of combustion was

assumed to be 226400 kJ and  $n$  was assumed to be 1 for all polymeric materials, based on the work of Friedman [15] and Henderson [5].

**Table II. Activation energy values as function of  $\alpha$ .**

$\alpha$	Ea (kJ/mol)	R <sup>2</sup>
0.4	212	0.9971
0.6	197	0.9971
0.8	195	0.999

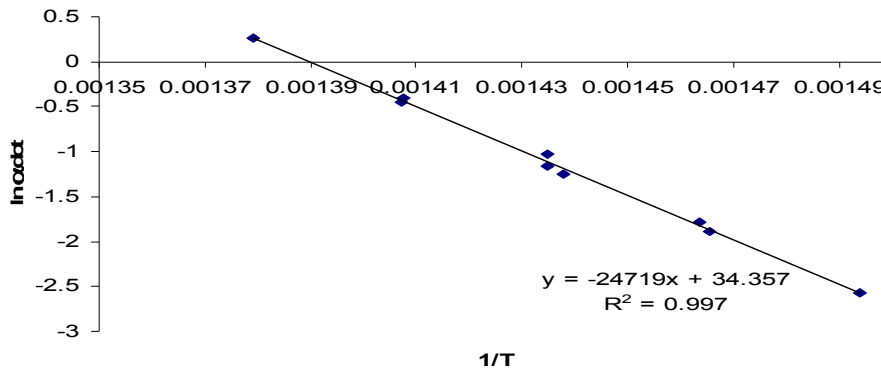


Figure 9. Plot of  $\ln \alpha \dot{}$  versus  $1/T$  for three different values of  $\alpha$  and the slope provides a value of  $B = -E/R$ .

Modelled mass loss curves were constructed using the measured mass loss rate and the derived decomposition rate parameters. Figure 10 shows a comparison between the measured and modelled mass loss curves for the CFRP NI epoxy laminate. The main but small deviation between experimental and theoretical analysis occurred during early degradation, where the calculated loss exceeded the actual weight loss. In conclusion the decomposition parameters are a reaction rate factor  $A$  equal to  $9.00 \times 10^{14}$  1/s and activation energy  $E$  equal to  $2.05 \times 10^5$  J/mol. These were sufficiently precise to be used in the thermal model.

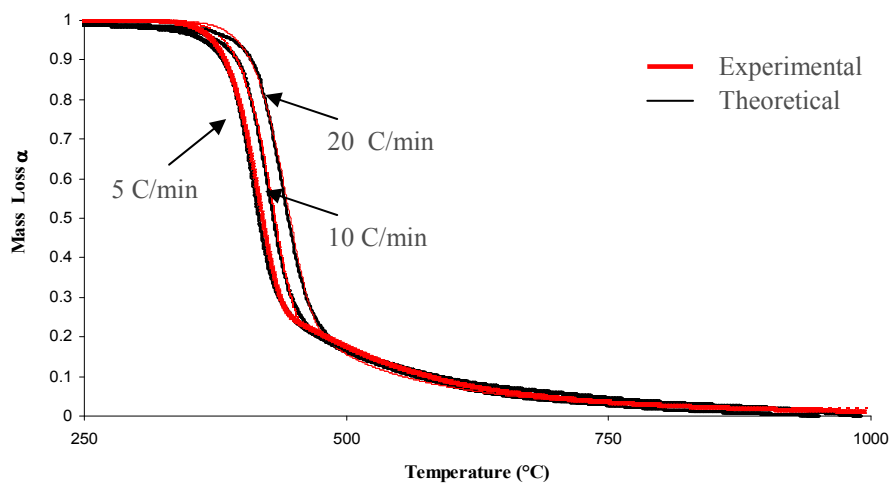


Figure 10. Measured and modelled mass loss curves for CFRP epoxy laminate exposed to a 5°C/min, 10°C/min and 20°C/min heating rates. The main decomposition region (350-480°C) is shown.

## 4.2 The Henderson Model

The Henderson equation has been adapted by Gibson et al. [10] and Dodds [9] to predict the fire performance of glass reinforced plastic laminates at different levels of heat flux :

$$\rho C_p \frac{\partial T}{\partial t} = \underbrace{\frac{\partial}{\partial x} \left( k \frac{\partial T}{\partial x} \right)}_{\text{Heat conduction}} - \underbrace{\dot{M}_G \frac{\partial}{\partial x} h_G}_{\text{Mass flow of volatile products}} - \underbrace{\rho A \left[ \frac{m - m_f}{m_o} \right]^n e^{\frac{-E}{RT}} (Q + h_c + h_r)}_{\text{Endothermic reaction of resin decomposition}} \quad (6)$$

Equation 6 shown the adapted model which has been simplified in a number of ways. The thermal conductivity and specific heat properties were assumed to remain constant with the increase in temperature. Thermal and gas transport properties were considered to be constant during the decomposition process. The three main processes involved in energy transfer described in equation 6 are: heat conduction through the material, the convective mass flow of volatile products and the endothermic reaction of resin decomposition. The model was used to predict the temperature profile versus time using finite difference techniques.

## 4.3 Thermal Model Temperature profile

Figure 15 compares the modelled and experimental rear face temperature profile for CFRP carbon epoxy laminate in 75kW/m<sup>2</sup> fire. This material was modelled reasonably well and the full temperature will be used to provide the necessary input for modelling the structural response of laminates in fire.

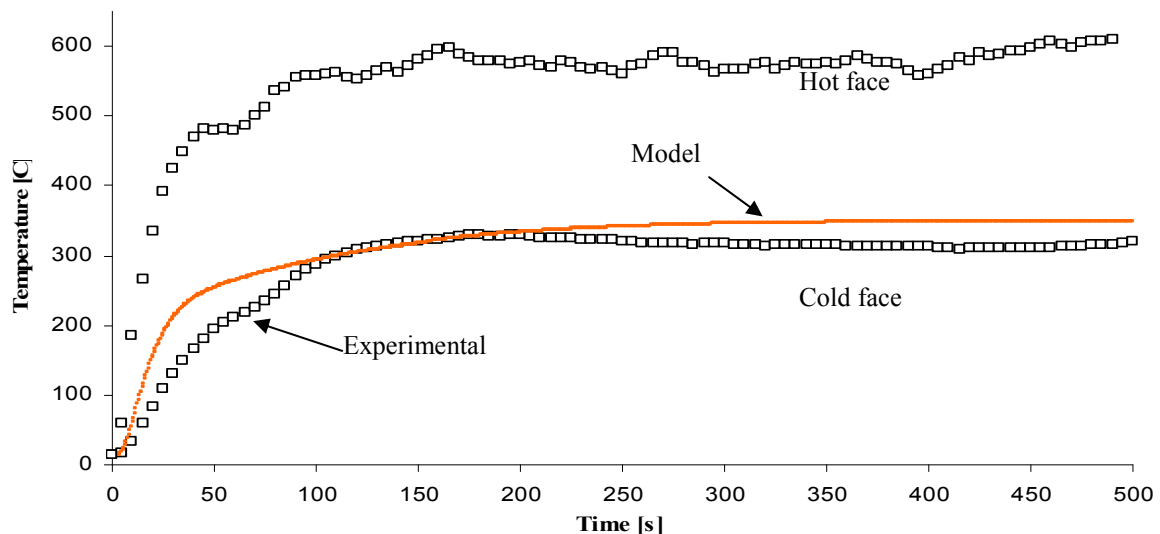


Figure 11. Predicted and measured temperature profiles for a 2 mm carbon epoxy laminate exposed to a 75kW/m<sup>2</sup> heat flux with natural convection and radiation on the cold face.

## 5.CONCLUSIONS

A number of conclusions can be drawn from the present study. A thermal model was based on TGA and thermal analysis. This enabled the temperature profile to be predicted for the carbon epoxy laminate. The response of the laminate and sandwich panels under fire and load was performed. The results showed that the unloaded laminate and sandwich panels met the (4-5 minutes) criteria required by FAA with respect to the burn-through thickness. However, when a high load was applied, the time to failure was significantly reduced. Although, this is a small scale test, it does nonetheless more accurately simulate the integrity of the material during a crash were fire and load are likely to be present. It would be interesting to assess the

same effects on a larger scale test. Considerably more work will need to be carried out in order to better predict the temperature profile for the sandwich panels due to the complexity of the sandwich panel construction. Future studies will focus on a structural model which will provide the time to failure of the materials tested.

## ACKNOWLEDGEMENTS

Research on integrity of composite materials in fire Newcastle University is funded by the **Marie Curie Momentum Research Training Network**.

## REFERENCES

- 1) Gibson, A.G., Wright, P.N.H., Wu, Y-S, Mouritz, A.P., Mathys, Z. and Gardiner, C.P. (2004). The Integrity of Polymer Composites During and After Fire, *J. of Composite Materials*, **38**: 15, 1283-1308, 2004.
- 2) Mouritz, A.P.(2006), Fire Safety of Advance Composite for Aircraft, Aviation Safety Research Grant B2004/0046, School of Aerospace, Mechanical & Manufacturing Engineering RMIT University.
- 3) CAP681 Global Fatal Accident Review 1980-1996. www.caa.co.uk
- 4) Fire and Smoke-Resistant Interiors Materials for Commercial Transport Aircraft (1995) The National Academy of Sciences.
- 5) Henderson, J.B., J.A. Wiebelt, and M.R. Tant, A Model for the thermal response of polymer composite materials with experimental verification. *Journal of Composite Materials*, 1985. 19: p. 579-594.
- 6) Gibson, A.G., et al., A model for the thermal performance of thick composite laminates in hydrocarbon fires. *Revue de l'Institut Français du Pétrole*, 1995. **50**(1): p. 69-74 (special issue).
- 7) Dao, M. and Asaro, R.J. (1999) A Study on Failure Prediction and Design Criteria for Fiber Composites under Fire Degradation', *Composites*, **30A**: 123-131.
- 8) Mouritz, A.P. and Mathys, Z. (2001) Post-Fire Mechanical Properties of Glass-Reinforced Polyester Composites, *Composites Science and Technology*, **61**: 475-490.
- 9) Dodds, N., et al., Fire behaviour of composite laminates. *Composites: Part A*, 2000. **31**(7): p. 689-702.
- 10) Gibson, A.G., et al. A Low Cost Burner Technique for the Development and Modelling of Laminates in Fire. in *Composites in Fire 3: 3rd International Conference on the Response of Composite Materials to Fire*. 2003. Newcastle upon Tyne, England.
- 11) Greene, E. (1993) Fire Performance of composite materials for naval applications, US Navy Contract N61533-91-C-0017, Structural Composites., Melbourne FL USA,
- 12) Gibson, A.G., et al., Laminate theory analysis of composites under load in fire. *Journal of Composite Materials*, 2006. **40**(7): p. 639-658.
- 13) Budiansky B. and N.A.Fleck (1993) Compressive Failure of Fibre Composite. *J.Mech.Phys.Solids* 41/1 183-211.
- 14) Schultheisz, R. and A.M.Waas (1996) Compressive Failure of Composite, Part I: Testing and Micromechanical Theories. *Prog. Aerospace Sci* 32:1-42.
- 15) Friedman, H.L. Kinetics of thermal degradation of char-forming plastics from thermogravimetry: Application to a phenolic plastic. in *Proceedings of the 136th American Chemical Society meeting*. 1959. Atlantic City, NJ.
- 16) Cai, X.E. ,Shen ,H., Zhang, C.H. , Wang ,Y.X. and Kong Z. (2000) Application of Constant Reaction Rate TG to the Determination of Kinetic Parameters by Hi-Res TG. *Journal of Thermal Analysis and Calorimetry* 60:623-628.
- 17) Opfermann, J.(2000) Kinetic analysis using multivariate non-linear regression. *Journal of Thermal Analysis and Calorimetry*. 60:641-658.